EUROGRAPHICS 2012 / P. Cignoni, T. Ertl
(Guest Editors)

Volume 31 (2012), Number 2

Advected Tangent Curves: A General Scheme for Characteristic Curves of Flow Fields

T. Weinkauf [1], H.-C. Hege [2], and H. Theisel [3]

[1] MPI Informatik, Saarbrücken, Germany — weinkauf@mpi-inf.mpg.de
[2] Zuse Institute Berlin, Berlin, Germany — hege@zib.de
[3] University of Magdeburg, Magdeburg, Germany — theisel@isg.cs.uni-magdeburg.de

Abstract

We present the first general scheme to describe all four types of characteristic curves of flow fields – stream, path, streak, and time lines – as tangent curves of a derived vector field. Thus, all these lines can be obtained by a simple integration of an autonomous ODE system. Our approach draws on the principal ideas of the recently introduced tangent curve description of streak lines. We provide the first description of time lines *as tangent curves of a derived vector field, which could previously only be constructed in a geometric manner. Furthermore, our scheme gives rise to new types of curves. In particular, we introduce* advected stream lines *as a parameter-free variant of the time line metaphor. With our novel mathematical description of characteristic curves, a large number of feature extraction and analysis tools becomes available for* all *types of characteristic curves, which were previously only available for stream and path lines. We will highlight some of these possible applications including the computation of time line curvature fields and the extraction of cores of swirling advected stream lines.*

Categories and Subject Descriptors (according to ACM CCS): I.3.3 [Computer Graphics]: Picture/Image Generation—Line and curve generation

1. Introduction

Flow fields play a vital role in many areas. Examples are burning chambers, turbomachinery and aircraft design in industry as well as blood flow in medicine. The motion of massless particles is governed by path lines in unsteady flows, and by stream lines in steady flows. A common approach to visualize flows in real-world experiments is to release dye, i.e., a large number of particles, into the flow and examine its behavior: vortices can be observed as patterns of swirling flow. The resulting dye structures are differentiated into two different types depending on how the dye was released. A *continuous* release of dye from a point, line, or surface leads to streak lines, streak surfaces or streak volumes. An *instantaneous* release, on the other hand, leads to time structures: a time line, for example, is created by releasing dye along a usually straight line for a single moment in time. The flow advects and deforms the time line, thereby elucidating intricate flow patterns. Stream, path, streak, and time lines are the classic characteristic curves of unsteady flows. In contrast to stream and path lines, streak and time lines have the ability to reveal vortex structures in the natural frame of reference (cf. Figure 7). This is one of the reasons why they are used so often in real-world experiments. In computer-based visualizations, on the other hand, stream and path lines have more applications due to their simpler mathematical background. In this paper, we will provide novel mathematical tools for time lines that will extend the possibilities for their analysis and visualization.

Stream and path lines have found their applications in integration-based as well as feature-based visualization methods. The latter build on the readily available differential descriptions of stream and path lines as tangent curves of certain vector fields, i.e., as solutions of autonomous ODE systems. This facilitates the mathematical analysis of stream and path lines, since their properties can be described by employing formulations that are purely based on the vector field and its derivatives. The integral curves themselves are not required. This gave rise to a large number of feature extraction and analysis methods such as the extraction of centers of swirling flow [PR99, WSTH07], or the computation of derived properties such as their curvature [WT02] *without actually integrating* a single stream or path line.

The situation is different for streak and time lines. Lacking a readily available differential description, they found their applications only in integration-based methods by means of geometric algorithms for their construction. For example, a number of recent contributions have been made

to use streak and time surfaces in interactive applications [CKSW08, FBTW10], compute them with high accuracy and surface quality [KGJ09], and to render them in a smoke-like manner to mimic real-world smoke experiments [vFWTS08]. These approaches have proven that streak and time lines/surfaces are valuable visualization tools for unsteady flows.

Only recently, a differential description of streak lines [WT10] has been introduced. It is based on the gradient of the flow map, which has to be computed numerically using a dense path line integration for all flows where the flow map is not given in a closed-form, e.g., numerically simulated flows. Algorithmically, this is similar to the computation of the Finite Time Lyapunov Exponent (FTLE) [Hal01]. This novel differential description of streak lines opened the gates to the large number of feature extraction and analysis tools that were previously only available for stream and path lines. Among the first applications were cores of swirling streak lines and streak line curvature fields [WT10]. Furthermore, significant speed-ups over the classic approach have been demonstrated for cases where a larger number of streak lines is to be computed.

In this paper, we provide the last missing differential description: we present the – to the best of our knowledge – first tangent curve description of time lines. Similar to the streak line approach from above, we define a new, derived *time line vector field* based on the gradient of the flow map. All tangent curves of this derived vector field are time lines of the original flow, and vice versa.

The new tangent curve description of time lines is part of a more general scheme developed in this paper. It builds on the notions of a *seeding field* and an *advection field*. Loosely speaking, a tangent curve of the former gets advected by the latter; yielding an *advected tangent curve* (Section 2). We will provide a differential description of advected tangent curves and show how this describes different kinds of characteristic curves depending on the specific choice for the seeding and advection field. In fact, our new concept encompasses all four classic types as well as new types of characteristic curves (Section 3). It enables new applications for time lines and surfaces (Section 4). Furthermore, we introduce a new type of characteristic curve called *advected stream lines*, which is a parameter-free variant of the time line metaphor. We discuss their properties and show their utility for feature-based and integration-based visualization methods (Section 5). Implementational issues are discussed in Section 6.

Our novel approach for representing and computing time lines has the following advantages over the classic geometric approach (similarly for advected stream lines):

- It enables feature-based analysis of times lines, since their inherent properties can now be described using the time line vector field and its derivatives.
- The computation of a larger number of time lines (or surfaces) is significantly faster.

Notation We consider a smooth n-dimensional ($n = 2,3$) time-dependent vector field $\mathbf{v}(\mathbf{x},t)$ over the domain $D \times T$ where $D \subseteq \mathbb{R}^n$ is the spatial domain and T is a time interval. We write derived $(n+1)$-dimensional variables with a bar like $\bar{\mathbf{p}}$, and derived $(n+2)$-dimensional variables with a double bar like $\bar{\bar{\mathbf{q}}}$. Locations in space-time are denoted as $\bar{\mathbf{x}} = (\mathbf{x},t)^T = (\mathbf{x},t)$. All vectors throughout the paper are column vectors, we often omit the explicit $()^T$ notation.

2. Advected Tangent Curves

This section presents the theoretical core of our approach: we define the concept of advected tangent curves as a generalization of all common characteristic curves of vector fields. Later we will show how this general concept can be applied to define vector fields whose tangent curves describe different characteristic curves of time-dependent flows.

2.1. Tangent Curves

Let $\mathbb{E}^n$ be the n-dimensional Euclidean space. A curve $L \subset \mathbb{E}^n$ is called a *tangent curve* of an n-dimensional vector field $\mathbf{v}(\mathbf{x})$, if for all points $\mathbf{p} \in L$ the tangent vector of L coincides with $\mathbf{v}(\mathbf{p})$. Tangent curves are the solutions of the autonomous ODE system

$$\frac{d}{d\tau}\mathbf{x}(\tau) = \mathbf{v}(\mathbf{x}(\tau)) \quad \text{with} \quad \mathbf{x}(0) = \mathbf{x}_0. \tag{1}$$

For all points $\mathbf{x} \in \mathbb{E}^n$ with $\mathbf{v}(\mathbf{x}) \neq \mathbf{0}$, there is one and only one tangent curve through it. They do not intersect or join each other. Hence, tangent curves uniquely describe the directional information of $\mathbf{v}$, which in turn allows to describe important properties of them solely by considering the derivatives of the vector field $\mathbf{v}$. This is the basis for many feature extraction and analysis methods such as the detection of vortex core lines [SH95, PR99, WSTH07], topological analysis [HH91], or the computation of scalar fields describing the curvature or torsion of tangent curves [WT02]. These methods rely entirely on the derivatives of $\mathbf{v}$ and can be applied *without* actually integrating a single tangent curve.

2.2. Conceptual Definition of Advected Tangent Curves

Let $\mathbf{v}(\mathbf{x},t)$ be the time-dependent vector field whose characteristic curves are to be analyzed. Additionally, we introduce two auxiliary $(n+1)$-dimensional vector fields:
the *advection field*

$$\bar{\mathbf{p}}(\bar{\mathbf{x}}) = \begin{pmatrix} \mathbf{w}(\mathbf{x},t) \\ 1 \end{pmatrix} \tag{2}$$

and the *seeding field*

$$\bar{\mathbf{f}}(\bar{\mathbf{x}}) = \begin{pmatrix} \mathbf{a}(\mathbf{x},t) \\ g(\mathbf{x},t) \end{pmatrix}. \tag{3}$$

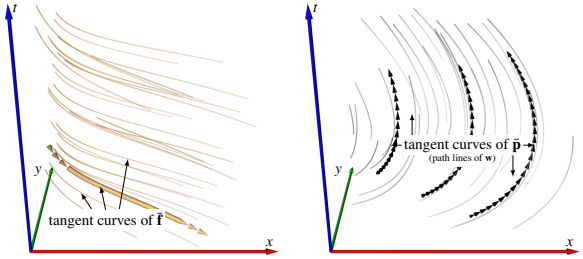

(a) Seeding field $\bar{\mathbf{f}}$. (b) Advection field $\bar{\mathbf{p}}$.

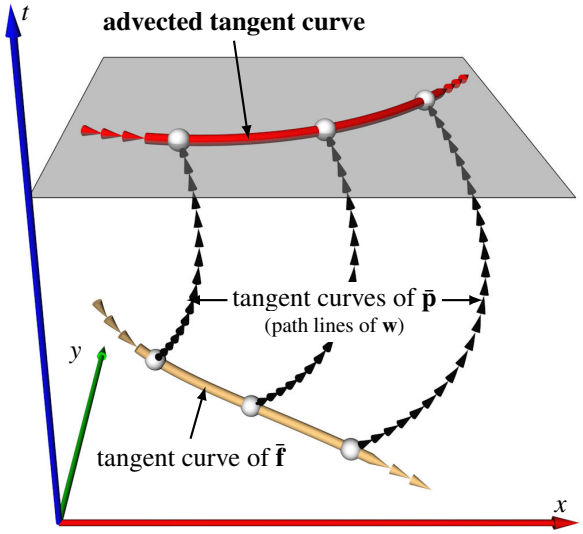

(c) Advected tangent curves (red) are created by advecting the tangent curves of $\bar{\mathbf{f}}$ (yellow) along the tangent curves of $\bar{\mathbf{p}}$ (black) until a time step t is reached.

Figure 1: *Conceptual definition of advected tangent curves.*

They consist of two time-dependent vector fields $\mathbf{w}(\mathbf{x},t)$ and $\mathbf{a}(\mathbf{x},t)$ as well as a time-dependent scalar field $g(\mathbf{x},t)$. In Section 3, we show that different choices of $\mathbf{w},\mathbf{a},g$ yield different characteristic curves of the vector field $\mathbf{v}$ to be analyzed. Note that the tangent curves of $\bar{\mathbf{p}}$ describe the path lines of $\mathbf{w}$ due to the last component being 1 [WT10]. In fact, later on we will rather often choose $\mathbf{w}=\mathbf{v}$ such that the advection field $\bar{\mathbf{p}}$ describes the particle motion of the underlying flow field $\mathbf{v}$.

We define advected tangent curves as follows:

Definition 1 Let L be a tangent curve of the seeding field $\bar{\mathbf{f}}$. Considering the set of particles of the advection field $\bar{\mathbf{p}}$ that run through L, the *advected tangent curve* L' is the collection of all these particles at a time t.

In other words, an advected tangent curve lives in the time step t and is created by advecting the original tangent curve of $\bar{\mathbf{f}}$ in the advection field $\bar{\mathbf{p}}$ until the time step t is reached. Geometrically, L' can be constructed as follows: choose a number of seed points on L, integrate tangent curves in $\bar{\mathbf{p}}$ starting from these seeds, and intersect the curves with the time t. Figure 1 illustrates the concept.

2.3. Flow Map of the Advection Field

To describe advected tangent curves in an algebraic manner, we need the flow map of the advection field $\bar{\mathbf{p}}$. The flow map $\phi : D \to D$ describes the spatial location of a particle seeded at $(\mathbf{x},t)$ and integrated over a time interval τ, denoted as $\phi_t^\tau(\mathbf{x})$. As a side note, the computation of Finite Time Lyapunov Exponents (FTLE) [Hal01] is essentially based on the consideration of the (spatial) gradient of ϕ. In fact, $\nabla\phi_t^\tau(\mathbf{x}) = \frac{\partial\phi}{\partial\mathbf{x}}$ is an $n\times n$ matrix describing the behavior of particles sent out in a small spatial neighborhood of $\mathbf{x}$. For our purposes, we additionally need the spatio-temporal, $(n+1)$-dimensional flow function $\bar{\phi}$ of $\bar{\mathbf{p}}$, which is defined as

$$\bar{\phi} : D\times T \to D\times T\ , \quad \bar{\phi}^\tau(\bar{\mathbf{x}}) = \begin{pmatrix}\phi_t^\tau(\mathbf{x})\\ t+\tau\end{pmatrix}. \tag{4}$$

The gradient of $\bar{\phi}$ can be expressed as the $(n+1)\times(n+1)$ matrix

$$\nabla\bar{\phi}^\tau(\bar{\mathbf{x}}) = \begin{pmatrix}\nabla\phi & \frac{\partial\phi}{\partial t}\\ 0\,..\,0 & 1\end{pmatrix}. \tag{5}$$

The fact, that the last component of $\bar{\mathbf{p}}$ is 1, ensures that the last line of $\nabla\bar{\phi}$ is $(0,..,0,1)$. Regarding the inverse of $\nabla\bar{\phi}$, we note

$$(\nabla\bar{\phi})^{-1} = \begin{pmatrix}\nabla\phi & \frac{\partial\phi}{\partial t}\\ 0...0 & 1\end{pmatrix}^{-1} = \begin{pmatrix}(\nabla\phi)^{-1} & -(\nabla\phi)^{-1}\cdot\frac{\partial\phi}{\partial t}\\ 0...0 & 1\end{pmatrix}. \tag{6}$$

2.4. Description of Advected Tangent Curves

We show that advected tangent curves can be expressed as tangent curves of a derived vector field:

Theorem 1 Given a seeding field $\bar{\mathbf{f}}$ and an advection field $\bar{\mathbf{p}}$ with its flow function $\bar{\phi}$, every advected tangent curve is a tangent curve of the $(n+2)$-dimensional vector field (and vice versa)

$$\bar{\mathbf{q}}(\bar{\mathbf{x}},\tau) = \begin{pmatrix}\left(\nabla\bar{\phi}\right)^{-1}\cdot\bar{\mathbf{f}}\left(\bar{\phi}\right) - g\left(\bar{\phi}\right)\cdot\bar{\mathbf{p}}\\ g\left(\bar{\phi}\right)\end{pmatrix} \tag{7}$$

in spatio-temporal notation with $\bar{\phi}=\bar{\phi}^\tau(\bar{\mathbf{x}})$ and $\bar{\mathbf{p}}=\bar{\mathbf{p}}(\bar{\mathbf{x}})$. Discriminating between spatial and temporal components, it reads

$$\bar{\mathbf{q}}(\mathbf{x},t,\tau) = \begin{pmatrix}(\nabla\phi)^{-1}\cdot\left(\mathbf{a}(\bar{\phi}) - g(\bar{\phi})\,\frac{\partial\phi}{\partial t}\right) - g(\bar{\phi})\cdot\mathbf{w}\\ 0\\ g(\bar{\phi})\end{pmatrix} \tag{8}$$

with $\phi=\phi_t^\tau(\mathbf{x})$, $\bar{\phi}=(\phi_t^\tau(\mathbf{x}),t+\tau)^T$ and $\mathbf{w}=\mathbf{w}(\mathbf{x},t)$, which follows directly from (2), (3) and (6). We call $\bar{\mathbf{q}}$ the *advected*

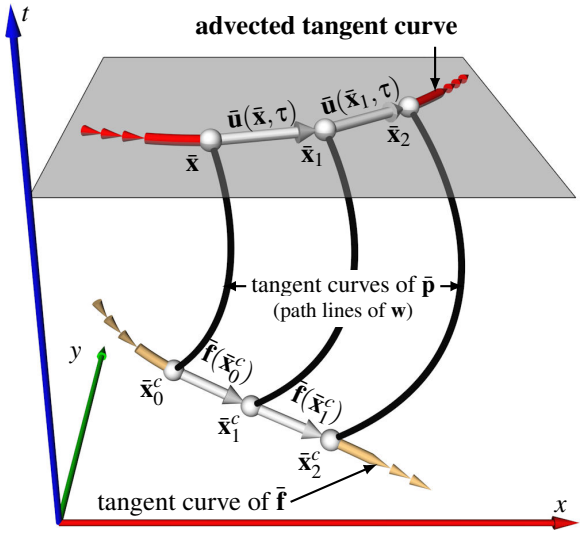

Figure 2: *Definition of the vector field $\bar{\mathbf{u}}(\bar{\mathbf{x}},\tau)$, which is the main ingredient of the advected tangent curve vector field $\bar{\bar{\mathbf{q}}}$.*

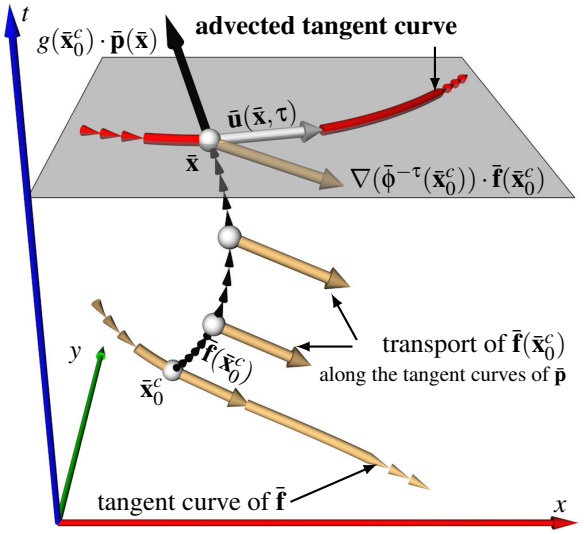

Figure 3: *Computing $\bar{\mathbf{u}}(\bar{\mathbf{x}},\tau)$ by transporting the seeding vector $\bar{\mathbf{f}}(\bar{\mathbf{x}}_0^c)$.*

tangent curve vector field. It is defined in the domain $D\times T\times\Upsilon$ with $\tau\in\Upsilon$.

Proof: Given is a certain advected tangent curve through the space-time point $\bar{\mathbf{x}}=(\mathbf{x},t)$ as shown in Figure 2. It relates to a point $\bar{\mathbf{x}}_0^c$ on the seeding tangent curve of $\bar{\mathbf{f}}$ via an integration in the advection field $\bar{\mathbf{p}}$. We can write this relation using the flow function in two ways, from the advected to the seeding tangent curve:

$$\bar{\mathbf{x}}_0^c=\bar{\phi}^{\tau}(\bar{\mathbf{x}})=\begin{pmatrix}\phi_t^{\tau}(\mathbf{x})\\ t+\tau\end{pmatrix}=\begin{pmatrix}\mathbf{x}_0^c\\ t+\tau\end{pmatrix}, \tag{9}$$

or from the seeding to the advected tangent curve:

$$\bar{\mathbf{x}}=\bar{\phi}^{-\tau}(\bar{\mathbf{x}}_0^c)=\begin{pmatrix}\phi_{t+\tau}^{-\tau}(\mathbf{x}_0^c)\\ t\end{pmatrix}=\begin{pmatrix}\mathbf{x}\\ t\end{pmatrix}. \tag{10}$$

The next point $\bar{\mathbf{x}}_1$ on the advected tangent curve can be obtained in the following way: integrate $\bar{\mathbf{f}}$ starting at the point $\bar{\mathbf{x}}_0^c$ for a small ε. From the resulting point $\bar{\mathbf{x}}_1^c$, do an integration of $\bar{\mathbf{p}}$ until the time t is reached:

$$\bar{\mathbf{x}}_1^c = \bar{\mathbf{x}}_0^c+\varepsilon\cdot\bar{\mathbf{f}}(\bar{\mathbf{x}}_0^c)=\begin{pmatrix}\mathbf{x}_1^c\\ t+\tau+\varepsilon\cdot g(\bar{\mathbf{x}}_0^c)\end{pmatrix} \tag{11}$$

$$\bar{\mathbf{x}}_1 = \bar{\phi}^{-\tau-\varepsilon\cdot g(\bar{\mathbf{x}}_0^c)}(\bar{\mathbf{x}}_1^c)=\begin{pmatrix}\mathbf{x}_1\\ t\end{pmatrix}. \tag{12}$$

To go from $\bar{\mathbf{x}}$ to $\bar{\mathbf{x}}_1$ by a vector field integration, we define the vector field

$$\bar{\mathbf{u}}(\bar{\mathbf{x}},\tau)=\lim_{\varepsilon\to 0}\frac{\bar{\mathbf{x}}_1-\bar{\mathbf{x}}}{\varepsilon}. \tag{13}$$

In order to observe the continuation of the advected tangent curve through $\bar{\mathbf{x}}$ and $\bar{\mathbf{x}}_1$, we consider another particle on the seeding tangent curve of $\bar{\mathbf{f}}$:

$$\bar{\mathbf{x}}_2^c = \bar{\mathbf{x}}_1^c+\varepsilon\cdot\bar{\mathbf{f}}(\bar{\mathbf{x}}_1^c)=\begin{pmatrix}\mathbf{x}_2^c\\ t+\tau+\varepsilon\cdot g(\bar{\mathbf{x}}_0^c)+\varepsilon\cdot g(\bar{\mathbf{x}}_1^c)\end{pmatrix} \tag{14}$$

$$\bar{\mathbf{x}}_2 = \bar{\phi}^{-\tau-\varepsilon\cdot g(\bar{\mathbf{x}}_0^c)-\varepsilon\cdot g(\bar{\mathbf{x}}_1^c)}(\bar{\mathbf{x}}_2^c)=\begin{pmatrix}\mathbf{x}_2\\ t\end{pmatrix}. \tag{15}$$

From this we can formulate $\bar{\bar{\mathbf{q}}}$ as

$$\bar{\bar{\mathbf{q}}}(\bar{\mathbf{x}},\tau)=\begin{pmatrix}\bar{\mathbf{u}}(\bar{\mathbf{x}},\tau)\\ g(\bar{\phi}^{\tau}(\bar{\mathbf{x}}))\end{pmatrix}. \tag{16}$$

In order to compute $\bar{\mathbf{u}}$, we observe how the vector $\bar{\mathbf{f}}(\bar{\mathbf{x}}_0^c)$ is transported under the integration of $\bar{\mathbf{p}}$ as shown in Figure 3. In fact, since an integration of $\bar{\mathbf{p}}$ over an integration time of $-\tau$ transports a particle from $\bar{\mathbf{x}}_0^c$ to $\bar{\phi}^{-\tau}(\bar{\mathbf{x}}_0^c)=\bar{\mathbf{x}}$ (cf. Equation (10)), the vector $\bar{\mathbf{f}}(\bar{\mathbf{x}}_0^c)$ is transported to $\nabla(\bar{\phi}^{-\tau}(\bar{\mathbf{x}}_0^c))\cdot\bar{\mathbf{f}}(\bar{\mathbf{x}}_0^c)$. Since the last line of $\nabla(\bar{\phi}^{-\tau}(\bar{\mathbf{x}}_0^c))$ is $(0,\ldots,0,1)$, the last component of $\nabla(\bar{\phi}^{-\tau}(\bar{\mathbf{x}}_0^c))\cdot\bar{\mathbf{f}}(\bar{\mathbf{x}}_0^c)$ is $g(\bar{\mathbf{x}}_0^c)$. This gives

$$\bar{\mathbf{u}}(\bar{\mathbf{x}},\tau)=\nabla(\bar{\phi}^{-\tau}(\bar{\mathbf{x}}_0^c))\cdot\bar{\mathbf{f}}(\bar{\mathbf{x}}_0^c)-g(\bar{\mathbf{x}}_0^c)\cdot\bar{\mathbf{p}}(\bar{\mathbf{x}}). \tag{17}$$

Applying the Nabla operator to both sides of the identity $\bar{\phi}^{-\tau}(\bar{\phi}^{\tau}(\bar{\mathbf{x}}))=\bar{\mathbf{x}}$, we get $\nabla\bar{\phi}^{-\tau}(\bar{\phi}^{\tau}(\bar{\mathbf{x}}))\cdot\nabla\bar{\phi}^{\tau}(\bar{\mathbf{x}})=I_{n+1}$ where I_{n+1} is the $(n+1)$ identity matrix. Inserting (9) into it gives

$$\nabla\bar{\phi}^{-\tau}(\bar{\mathbf{x}}_0^c)=(\nabla\bar{\phi}^{\tau}(\bar{\mathbf{x}}))^{-1}. \tag{18}$$

Inserting this and (9) into (17), and the result into (16) gives the desired spatio-temporal formula (7) for $\bar{\bar{\mathbf{q}}}$.

3. Characteristic Curves as Advected Tangent Curves

In the following, we apply the methodology from the previous section and show how different types of characteristic

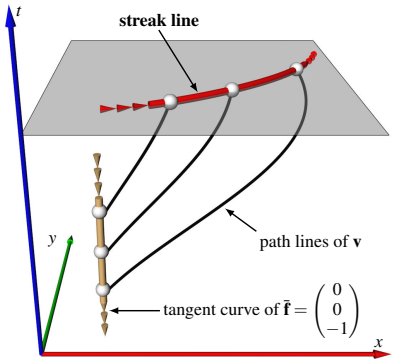

Figure 4: *Streak lines.*

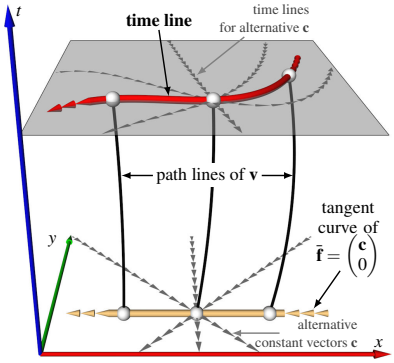

Figure 5: *Time lines.*

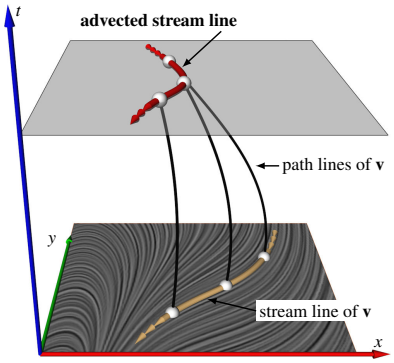

Figure 6: *Advected stream lines.*

curves can be described as advected tangent curves. This includes classic and new types of curves.

3.1. Classic Types of Characteristic Curves

Stream, path, streak, and time lines are the four classic types of characteristic curves in time-dependent flows. While tangent curve descriptions for stream and path lines are trivial, this is not the case for streak and time lines. Only recently, a tangent curve description for streak lines has been introduced [WT10]. It allows to apply feature extraction and analysis methods to streak lines that have been developed in our community originally for stream or path lines, but could not be applied to streak lines since their inherent properties could not be described in terms of the derivatives of some vector field. As we will show in the following, the streak line description of [WT10] is a special case of the advected tangent curve scheme from Section 2. Our more general scheme covers all four classic types of characteristic curves.

Time Lines $\boxed{\mathbf{w} = \mathbf{v}, \mathbf{a} \equiv \mathbf{c}, g \equiv 0}$

A time line is the collection of all particles seeded along a straight line at the same time step, i.e., a straight line which gets advected by the flow. An analogue in the real world is an infinitely flexible yarn or wire thrown into a river, which gets transported and deformed by the flow. Geometrically, a time line can be obtained by applying a path surface integration in the flow field starting at a straight line with $t = \text{const}$, and intersecting the path surface with a hyperplane perpendicular to the t-axis. Note that some definitions in the literature do not require the seeding line to be straight. As shown in Section 3.2, our approach works also for non-straight seeding lines as long as they can be described by (3).

To provide a differential description for the time lines of a time-dependent flow field $\mathbf{v}(\bar{\mathbf{x}})$, we apply our new method for advected tangent curves from Section 2 as follows:

- The seeding field $\bar{\mathbf{f}}$ is chosen such that it describes straight lines living in a constant time step, i.e., we set $\mathbf{a} \equiv \mathbf{c}, g \equiv 0$ where $\mathbf{c}$ is a constant vector. We have
$$\bar{\mathbf{f}}(\bar{\mathbf{x}}) = \begin{pmatrix} \mathbf{c} \\ 0 \end{pmatrix}. \tag{19}$$
- The advection field $\bar{\mathbf{p}}$ is chosen such that it describes the path lines of the flow field $\mathbf{v}$, i.e., we set $\mathbf{w} = \mathbf{v}$ and have
$$\bar{\mathbf{p}}(\bar{\mathbf{x}}) = \begin{pmatrix} \mathbf{v}(\bar{\mathbf{x}}) \\ 1 \end{pmatrix}. \tag{20}$$

Inserting these choices into (8) gives the *time line vector field*

$$\bar{\bar{\mathbf{q}}}(\mathbf{x}, t, \tau) = \begin{pmatrix} \left(\nabla \phi_t^\tau(\mathbf{x})\right)^{-1} \cdot \mathbf{c} \\ 0 \\ 0 \end{pmatrix}. \tag{21}$$

Figure 5 illustrates this. To the best of our knowledge, this is the first description of time lines as tangent curves of a derived vector field.

Note that different constant vectors $\mathbf{c}$ yield different time lines. In other words, the time line vector field is parameter-dependent. We will detail its properties in Section 4.

Streak Lines $\boxed{\mathbf{w} = \mathbf{v}, \mathbf{a} \equiv \mathbf{0}, g \equiv -1}$

A streak line is the connection of all particles set out at different times but the same point location. In an experiment, one can observe these structures by constantly releasing dye into the flow from a fixed position. The resulting streak line consists of all particles which have been at this fixed position sometime in the past. Geometrically, streak lines can be obtained by applying a path surface integration starting from a straight line parallel to the t-axis, and intersecting this path surface with a hyperplane perpendicular to the t-axis.

Streak lines can be described as tangent curves of a derived vector field using a constant seeding field $\bar{\mathbf{f}}$ pointing backwards in time and an advection field $\bar{\mathbf{p}}$ describing the path lines of the flow (Figure 4):

$$\bar{\mathbf{f}}(\bar{\mathbf{x}}) = \begin{pmatrix} \mathbf{0} \\ -1 \end{pmatrix} \qquad \bar{\mathbf{p}}(\bar{\mathbf{x}}) = \begin{pmatrix} \mathbf{v}(\bar{\mathbf{x}}) \\ 1 \end{pmatrix}. \tag{22}$$

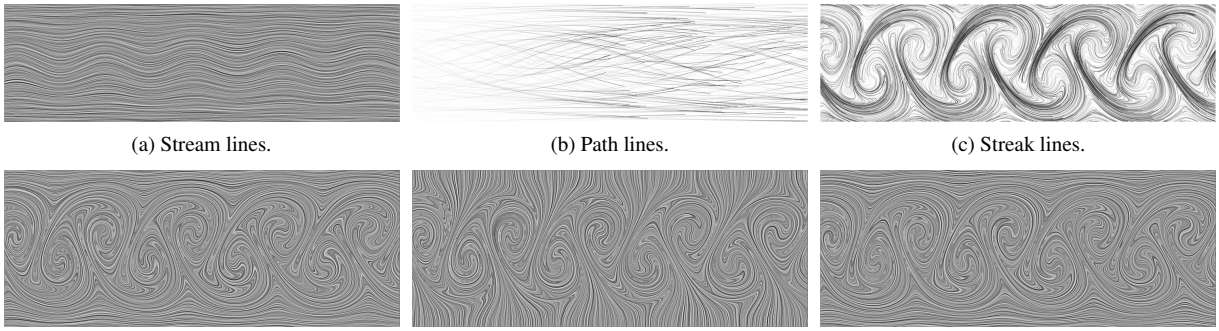

(a) Stream lines. (b) Path lines. (c) Streak lines.

(d) Time lines for two different constant vectors **c**. The differences at the upper and lower border of the images are induced by the choice of **c**. (e) Advected stream lines.

Figure 7: *Overview of different characteristic curves in the 2D time-dependent flow behind a cylinder. All curves are shown in the same spatial domain downstream from the cylinder where the well-known von Kármán vortex street is well developed. Time step and τ are the same for stream lines, time lines, and advected stream lines. Path and streak lines are defined over a time or τ-interval, which have been chosen to match the other curves as much as possible.*

Inserting these choices into (8) gives the *streak line vector field* as it is already known from [WT10]

$$\bar{\tilde{\mathbf{q}}}(\mathbf{x},t,\tau) = \begin{pmatrix} \left(\nabla\phi_t^\tau(\mathbf{x})\right)^{-1} \cdot \frac{\partial\phi_t^\tau(\mathbf{x})}{\partial t} + \mathbf{v}(\mathbf{x},t) \\ 0 \\ -1 \end{pmatrix}. \qquad (23)$$

Hence, the theory regarding streak lines from [WT10] is a special case of the more general scheme that we introduced in Section 2. We refer the reader to [WT10] for a detailed discussion of streak lines.

Stream and Path Lines

Path lines describe the trajectories of massless particles in time-dependent vector fields, whereas stream lines do the same in steady vector fields. Both can be described as tangent curves of a derived vector field in a straightforward fashion. The stream lines of a time-dependent flow **v** are given as the tangent curves of $\bar{\mathbf{s}} = (\mathbf{v}, 0)$. The path lines of **v** are the tangent curves of $\bar{\mathbf{p}} = (\mathbf{v}, 1)$.

Hence, it is not necessary to describe stream and path lines as advected tangent curves. However, from a theoretical point of view, it is interesting to see that they fit into our general scheme as well. Equation (8) describes stream lines for $\mathbf{w} \equiv \mathbf{0}$, $\mathbf{a} = \mathbf{v}, g \equiv 0$, and path lines for $\mathbf{w} \equiv \mathbf{0}$, $\mathbf{a} = \mathbf{v}, g \equiv 1$.

As a side note, considering Equation (8) for a *steady* vector field confirms the commonly known fact that path and streak lines coincide with stream lines in this case, whereas time lines do not.

3.2. New Types of Characteristic Curves

The general scheme of advected tangent curves does not only provide tangent curve descriptions of the four classic types of characteristic curves, but it gives also rise to new ones. It turns out that generalized streak lines [WTS*07] can be described using this scheme – in order to focus on our core contributions, we detail this only in the supplemental material. In the following we will introduce *advected stream lines* as a parameter-independent alternative to time lines.

Advected Stream Lines $\boxed{\mathbf{w} = \mathbf{v}, \mathbf{a} = \mathbf{v}, g \equiv 0}$

As described earlier, time lines depend on the choice of a constant vector **c** that defines the direction of the straight seeding lines. In fact, for every given time-dependent flow, there is a family of time line vector fields describing different time lines for different choices of **c**.

We propose a parameter-independent alternative that is seeded from curves at a constant time step – just like time lines –, but these curves are not straight lines anymore. In particular, we propose to advect the stream lines of a time-dependent flow **v** along its path lines. We set

$$\bar{\tilde{\mathbf{f}}}(\bar{\mathbf{x}}) = \begin{pmatrix} \mathbf{v}(\bar{\mathbf{x}}) \\ 0 \end{pmatrix} \qquad \bar{\tilde{\mathbf{p}}}(\bar{\mathbf{x}}) = \begin{pmatrix} \mathbf{v}(\bar{\mathbf{x}}) \\ 1 \end{pmatrix} \qquad (24)$$

for the seeding and the advection field, respectively. Figure 6 gives an illustration. We call this new class of characteristic curves *advected stream lines*. Their tangent curve description is given by inserting (24) into (8) and reads

$$\bar{\tilde{\mathbf{q}}}(\mathbf{x},t,\tau) = \begin{pmatrix} \left(\nabla\phi_t^\tau(\mathbf{x})\right)^{-1} \cdot \mathbf{v}(\phi_t^\tau(\mathbf{x}), t+\tau) \\ 0 \\ 0 \end{pmatrix}. \qquad (25)$$

We will detail their properties in Section 5.

4. Time Lines

4.1. Seeding and Integration

The time line vector field $\bar{\tilde{\mathbf{q}}}(\mathbf{x},t,\tau)$ from Equation (21) can be used as follows to integrate a time line which corresponds

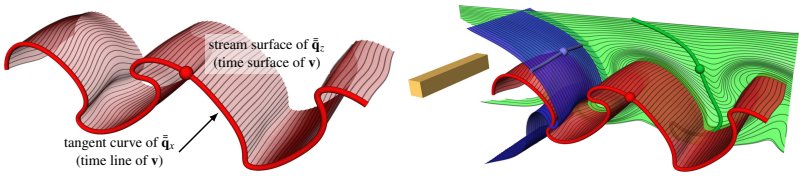

(a) Computing a time surface as a stream surface using two time line vector fields of the same flow $\mathbf{v}$, but corresponding to different seeding fields.

(b) Time surfaces computed using the pairs $(\bar{\mathbf{q}}_x, \bar{\mathbf{q}}_z)$ (red), $(\bar{\mathbf{q}}_z, \bar{\mathbf{q}}_y)$ (blue), and $(\bar{\mathbf{q}}_y, \bar{\mathbf{q}}_x)$ (green).

Figure 8: *Time surfaces in the flow behind a square cylinder at $t = 100$ and $\tau = -5$. After pre-computing the time line vector fields (4 minutes each), the time surfaces can be integrated in a fraction of a second.*

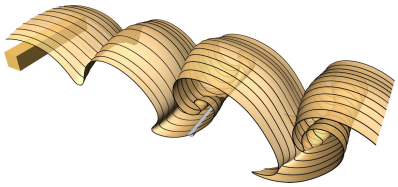

Figure 9: *Advected stream surface in the flow behind a square cylinder at $t = 100$ and $\tau = -10$. After pre-computing $\bar{\bar{\mathbf{q}}}$ (8 minutes), the advected stream surfaces can be integrated at interactive rates since they are stream surfaces of $\bar{\bar{\mathbf{q}}}$.*

to the straight line planted into the flow at t_0 and transported over a time interval τ:

1. Seed a tangent curve at $(\mathbf{x}, t_0 + \tau, -\tau)$.
2. Integrate $\bar{\bar{\mathbf{q}}}$ in forward and backward direction. Since the integration will stay in the same t,τ-slices (the last two components of $\bar{\bar{\mathbf{q}}}$ are zero), it suffices to keep the spatial subspace in memory.

All visualization methods for steady vector fields are suitable for the depiction of time lines, since for a given choice of t and τ the time line vector field reduces to a steady n-dimensional vector field. For example, the time lines of a 2D time-dependent flow can be visualized using Line Integral Convolution (LIC) applied to a spatial subspace of $\bar{\bar{\mathbf{q}}}$. Figure 7d shows this for a flow behind a cylinder. This data set has been simulated using the Free Software *Gerris Flow Solver* [Pop04]. Note that the stream and path lines of this flow (Figures 7a-b) do not reveal the patterns of the well-known von Kármán vortex street, whereas time lines, streak lines, and advected stream lines do.

Integrating a time line in $\bar{\bar{\mathbf{q}}}$ amounts to a simple tangent curve integration, whereas the classic approach amounts to a path surface integration. Comparing the two approaches, the time spent for computing $\bar{\bar{\mathbf{q}}}$ will be amortized for a certain number of time lines. In our implementation, this happens for the 2D cylinder flow at around 300 time lines. After that, our new approach is faster. Similar statements apply to time surfaces and advected stream lines/surfaces. See the supplemental material for more details.

A time surface of a 3D time-dependent flow is the collection of all particles seeded from a planar surface patch. Typically, a time surface is computed by advecting the surface patch through the flow, thereby exposing it to diverging/converging flow behavior. In principal, the *whole surface* has to be checked after every integration step for its compliance with given resolution and quality constraints. Only recently, a number of solutions have been presented to deal effectively and efficiently with this problem [vFWTS08, KGJ09, FBTW10]. Using the tangent curve description of time lines, time surfaces can now be integrated as stream surfaces in $\bar{\bar{\mathbf{q}}}$ using one of many well-established algorithms, e.g., [Hul92]. The advantage is that one only needs to check the *front line* of the stream surface for insertion/removal of tracers during integration.

An arbitrary seeding curve cannot be used for this stream surface, since the result will generally not correspond to a planar surface patch at $\tau = 0$. We give the following algorithm for computing time surfaces using two time line vector fields $\bar{\bar{\mathbf{q}}}_1$ and $\bar{\bar{\mathbf{q}}}_2$, which have been obtained using two different constant vectors $\mathbf{c}_1$ and $\mathbf{c}_2$ for the seeding field:

1. Integrate a time line as a tangent curve in $\bar{\bar{\mathbf{q}}}_1$.
2. Starting from this line, integrate a stream surface in $\bar{\bar{\mathbf{q}}}_2$.

The result is a time surface that corresponds to a planar surface patch spanned by $\mathbf{c}_1$ and $\mathbf{c}_2$ at $\tau = 0$. An illustration is shown in Figure 8a. The red seeding time line has been integrated in the time line vector field $\bar{\bar{\mathbf{q}}}_x$ defined by $\mathbf{c}_x = (1,0,0)^T$, and the semi-transparent time surface has been integrated as a stream surface in $\bar{\bar{\mathbf{q}}}_z$ defined by $\mathbf{c}_z = (0,0,1)^T$. Further time surfaces of this flow behind a square cylinder are shown in Figure 8b. This data set is a direct numerical Navier Stokes simulation by Camarri and Salvetti (U Pisa), Buffoni (Politecnico of Torino), and Iollo (U Bordeaux I) [CSBI05]. It is an incompressible solution with a Reynolds number of 200.

4.2. Feature Extraction and Analysis

The tangent curve description of time lines facilitates their mathematical analysis and opens the door to a number of feature extraction and analysis methods that were previously only available for stream, path, and streak lines.

Equation (21) suggests a relation between FTLE and time lines since both utilize the spatial gradients of ϕ. As it turns out, in vector fields for which $\nabla\phi$ is the identity, we have it that FTLE is zero and time lines are straight lines. This is for example the case in the *Beads Problem* flow: Wiebel et al. [WCW*11] reported of a biofluid dynamic model where

neither classic visualization methods such as LIC or path lines, nor feature extraction methods such as vector field topology or FTLE were able to detect an apparent attractor in the flow, i.e., a point in the flow where particles aggregate. Wiebel et al. used particle density to extract the attractor. Since the simulation is not available to us, we use an analytic variant [Pei09] of this flow which exhibits similar properties:

$$\mathbf{v}(x,y,t) = \begin{pmatrix} -(y - \frac{1}{3}\sin(t)) - (x - \frac{1}{3}\cos(t)) \\ (x - \frac{1}{3}\cos(t)) - (y - \frac{1}{3}\sin(t)) \end{pmatrix}. \quad (26)$$

Since this is a time-periodic flow, the attractor can be found using the method of Shi et al. [STW*06]. It is a path line with the following parametric description:

$$\mathbf{x}(t) = \frac{1}{3}\left(\sin(t) + \cos(t), -\cos(t) + \sin(t)\right)^T. \quad (27)$$

Figure 11c reveals that the time lines of this flow are straight lines – even for long integration times τ. Hence, the attractor cannot be found using time lines, which therefore will most likely not play a role in an unsteady topology.

Another remarkable property is that the time line vector field cannot have zeros, i.e., the spatial projection of $\bar{\bar{\mathbf{q}}}$ (often visualized using LIC in this paper) cannot have critical points. This can be seen as follows: Note that both the seeding and the advection field for the time line case do not have critical points. Consider now two neighboring particles at $\tau = 0$. During the advection, they can come very close to each other, but they can never coincide, since their movement is given by path lines which are tangent curves in space-time, and tangent curves cannot intersect each other (Section 2.1). Mathematically, this can also be seen using the Cauchy stress tensor $\nabla\phi^T\nabla\phi$ which describes the behavior of neighboring particles: it is always positive definite.

For every point in the $(n+2)$-dimensional time line vector field there is one and only one time line through it. This allows to define derived scalar fields describing time line properties just by considering the derivatives of $\bar{\bar{\mathbf{q}}}$. Integrating the time lines themselves is not required. For example, we can compute the curvature of time lines as a scalar field:

$$\kappa_{2D}(\mathbf{u}) = \frac{\det(\mathbf{u}, \nabla\mathbf{u}\cdot\mathbf{u})}{\|\mathbf{u}\|^3} \quad , \quad \kappa_{3D}(\mathbf{u}) = \frac{\|\mathbf{u}\times\nabla\mathbf{u}\cdot\mathbf{u}\|}{\|\mathbf{u}\|^3} \quad (28)$$

for 2D and 3D flows respectively, and with $\mathbf{u}$ denoting the spatial projection of $\bar{\bar{\mathbf{q}}}$. Figure 10 (top) shows the curvature of time lines.

5. Advected Stream Lines

5.1. Seeding and Integration

Advected stream lines are integrated as tangent curves in $\bar{\bar{\mathbf{q}}}(\mathbf{x},t,\tau)$ from Equation (25) as described earlier for time lines. In contrast to time lines, however, advected stream lines do not depend on a parameter. They are uniquely defined for a time-dependent flow $\mathbf{v}$. They can be visualized, similar as time lines, using e.g. LIC. See Figures 7e and 11d.

An advected stream surface S_A is the collection of all particles started from a regular stream surface S of the underlying flow and integrated over a certain time interval τ. S_A can be computed as a stream surface in $\bar{\bar{\mathbf{q}}}$. In contrast to time surfaces, any seeding curve can be used. This can be seen by noting that S_A is a family of advected stream lines. They correspond to a family of regular stream lines at $\tau = 0$, which give the regular stream surface S of the underlying flow. Figure 9 shows an advected stream surface.

5.2. Feature Extraction and Analysis

Areas where characteristic curves of a flow exhibit a spiraling behavior are of great interest since they are usually associated with important flow features such as vortices. Sujudi and Haimes developed a method of 3D steady flows to extract core lines around which stream lines swirl [SH95]. The Parallel Vectors operator is often used to extract these features [PR99]. For 3D time-dependent flows, one may track these core lines over time [TSW*05], which yields surfaces in the 4D space-time domain. However, since the motion in unsteady flows is governed by path lines, it seems reasonable to investigate their swirling motion as done in [WSTH07]. This yields surfaces in the 4D space-time domain, too.

In this section we want to extend the same idea to advected stream lines and extract cores around which they show spiraling behavior. Since their geometry is governed by the motion of particles, a spiraling behavior of advected stream lines indicates the presence of a vortex.

Let us first consider a 2D time-dependent flow $\mathbf{v}$ with its 4D advected stream line vector field $\bar{\bar{\mathbf{q}}}$. Let $\mathbf{u}$ be the spatial projection of $\bar{\bar{\mathbf{q}}}$, which is a 2D vector field for a certain choice of (t,τ). It has been shown in [WSTH07] that the approach of Sujudi/Haimes essentially degrades to tracking critical points in such 2D vector fields. We follow this idea and define the *cores of swirling advected stream lines* as the collection of all critical points of $\mathbf{u}$ over all (t,τ) under the side condition that $\nabla\mathbf{u}$ has a pair of complex eigenvalues. This side condition ensures swirling behavior of the advected stream lines around the core. The cores are surface structures in the 4D domain of $\bar{\bar{\mathbf{q}}}$. In space-time or $D\times\Upsilon$, they are lines.

Figure 11b shows such a core in space-time for $\tau = -9$ in the Beads Problem flow. As it turns out, the core line approaches the attractor with decreasing τ. This is an interesting result, since the Beads problem is considered to be one of the major test cases for a successful approach to an unsteady flow topology. Gathering the results from Wiebel et al. [WCW*11], Weinkauf and Theisel [WT10] and this paper, we have the following situation regarding the attractor in the Beads Problem flow: the cores of swirling stream and

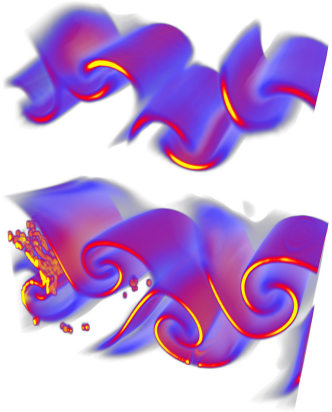

Figure 10: *Volume renderings of the curvature of time lines (top, $\tau = -5$) and advected stream lines (bottom, $\tau = -10$) in the flow behind a square cylinder at $t = 100$.*

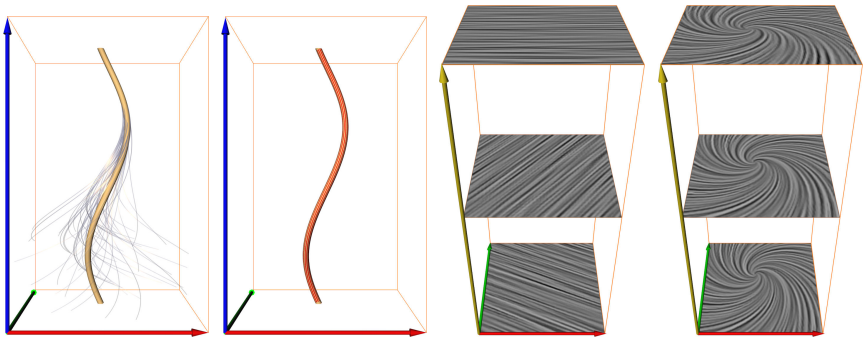

(a) Path lines in the vicinity of the attractor (yellow curve). From [WT10].

(b) Advected stream line core (red) matches the attractor at $\tau = -9$.

(c) Time lines are straight lines. $D \times \Upsilon$ domain with $\tau = (-9, 0)$.

(d) Advected stream lines in the $D \times \Upsilon$ domain with $\tau = (-9, 0)$.

Figure 11: *Time lines are straight lines in the* Beads Problem *flow since the gradient of the flow map $\nabla\phi$ is the identity. Advected stream lines, on the other hand, reveal the distinct flow behavior, and the core of swirling advected stream lines matches the attractor.*

path lines do not match it, time lines do not exhibit features following the notion of Sujudi/Haimes, but streak line cores and advected stream line cores can be used to find the attractor reliably. Further investigations of this topic are left to future research.

As a side note, the cores of advected stream lines can also be obtained by first tracking the critical points of the original flow $\mathbf{v}$ in space-time, and then advecting these line-type structures along the path lines of $\mathbf{v}$. This follows directly from the definition of advected stream lines.

The approach for 3D time-dependent flows follows along the same lines, but yields volumes in 5D. Since the spatial projection $\mathbf{u}$ is a steady 3D field, one could also apply the original approach of Sujudi/Haimes to this field, i.e., search for core lines where $\mathbf{u} \parallel \nabla\mathbf{u} \cdot \mathbf{u}$ in regions where $\nabla\mathbf{u}$ has complex eigenvalues. We leave this for future research.

Similarly to time lines, we can compute the curvature of advected stream lines as a derived scalar field. Figure 10 (bottom) shows this for the flow behind a square cylinder.

6. Implementation and Evaluation

6.1. Implementation

We discuss the implementation here only for the 2D time-dependent case, but it extends to 3D in a straightforward fashion. We compute the advected tangent curve vector field or one of its variants on an $n_x \times n_y \times n_T \times n_\tau$ 4D grid, where (n_x, n_y, n_T) denotes the grid resolution of the original flow and $n_\tau = n_T$, as follows:

1. For every grid point $(x_i, y_i, t_i, 0)$ of $\bar{\bar{\mathbf{q}}}$, seed four path lines in the spatial ε-neighborhood $(x_i \pm \varepsilon, y_i, t_i, 0)$, $(x_i, y_i \pm \varepsilon, t_i, 0)$ to approximate the spatial gradients of the flow map, and two path lines in the temporal ε-neighborhood $(x_i, y_i, t_i \pm \varepsilon, 0)$ to do the same for the temporal gradients. Note that some of the variants of $\bar{\bar{\mathbf{q}}}$ require only a subset of these computations, e.g., for time lines and advected stream lines it suffices to compute the spatial gradients.
2. Integrate the path lines until they leave the domain $D \times T$.
3. Intersect these path lines with every time step t_j and compute $\bar{\bar{\mathbf{q}}}$ as given in (8). Assign the result to the grid point (x_i, y_i, t_i, τ_j) where $\tau_j = t_i - t_j$. If one of the path lines left the domain before reaching t_j, denote this grid point to be invalid (e.g., assign zeros). This applies in particular to all boundary grid points since some of their seeds are already outside of the domain.

Note that the last two components of $\bar{\bar{\mathbf{q}}}$ are constant for most types of characteristic curves. In these cases, it suffices to save the first two components of $\bar{\bar{\mathbf{q}}}$ and add the constant components later on-the-fly during integration.

6.2. Numerical Accuracy

We evaluated the numerical accuracy of an integration in the advected tangent curve vector field $\bar{\bar{\mathbf{q}}}$ using analytical and numerical ground truths similar to the ones that have been used by Weinkauf and Theisel [WT10] for the evaluation of the streak line vector field. We found the same high accuracy as reported in [WT10]. This is not surprising since the advected tangent curve vector field uses the same numerical ingredients – spatial and temporal derivatives of the flow map – as the streak line vector field. In fact, the streak line vector field is a special case of the approach presented in this paper. The interested reader is referred to [WT10] for a detailed analysis of this issue.

6.3. Memory Requirements

Assuming the time-dependent vector field $\mathbf{v}(\mathbf{x},t)$ has n_T time steps, each of them requiring the amount of memory M, then the vector fields for time and advected stream lines require:

- M, the equivalent of a single time step, if we explore the curves for a given (t,τ). Examples of this are shown using LIC images throughout the paper.
- $n_T \cdot M$, the equivalent of the original flow, if we stay within a given time step t_0 or a given τ.
- $n_T^2 \cdot M$ to cover the whole space.

More details are given in the supplemental material.

6.4. Computation Times

Computing $\bar{\bar{\mathbf{q}}}$ for a time step of the 2D cylinder data set took 52 seconds single-threaded on a laptop with an Intel Core 2 Duo T9550 (2.66GHz). Computing a spatial slice of the time line or advected stream line vector fields took 4 minutes for an integration interval $\tau = -5$ in the 3D time-dependent flow around a square cylinder. More measurements are given in the supplemental material. All approaches based on flow maps, such as FTLE or our advected tangent curves, spend a significant amount of time with computing the flow map and should benefit from faster approximation schemes such as [BR10, HSW11]. We leave it to future work to investigate this in detail.

7. Conclusions and Future Work

We introduced the – to the best of our knowledge – first differential description of time lines. This is based on the novel concept of advected tangent curves, which provides for the first time differential descriptions of all classic characteristic curves in a combined setting. It also allows for new types of curves such as the newly introduced advected stream lines. Our work in this paper focuses on the theoretical aspects of characteristic curves in general. There is still room for improvement of practical issues such as the memory consumption and the computation times of $\bar{\bar{\mathbf{q}}}$. While our differential descriptions are not meant to replace the previous geometric approaches for computing time and streak lines/surfaces, they provide two major advantages: They are significantly faster if a larger number of integral lines/surfaces has to be computed. But most importantly, they allow to describe the properties of these lines by means of $\bar{\bar{\mathbf{q}}}$ and its derivatives without actually integrating them. This opens the gate to the large number of feature extraction and analysis tools that have been developed in the visualization community for stream and path lines – a promising avenue for future research. We made a first step into this direction and introduced the first feature-based approaches for time and advected stream lines: curvature scalar fields and advected stream line cores. We already mentioned other future research directions throughout the paper. As a last note, we only investigated a specific set of seeding and advection fields, and it may be of interest to look into other choices in order to explore the space of curves provided by our approach.

Acknowledgments

We thank Torsten Möller (Simon Fraser University, Vancouver) for his insightful comments.

References

[BR10] BRUNTON S. L., ROWLEY C. W.: Fast computation of finite-time Lyapunov exponent fields for unsteady flows. *Chaos 20*, 1 (2010), 017503. 10

[CKSW08] CUNTZ N., KOLB A., STRZODKA R., WEISKOPF D.: Particle level set advection for the interactive visualization of unsteady 3D flow. *Computer Graphics Forum (Proc. Eurovis) 27*, 3 (2008), 719–726. 2

[CSBI05] CAMARRI S., SALVETTI M.-V., BUFFONI M., IOLLO A.: Simulation of the three-dimensional flow around a square cylinder between parallel walls at moderate reynolds numbers. In *XVII Congresso di Meccanica Teorica ed Applicata* (2005). 7

[FBTW10] FERSTL F., BÜRGER K., THEISEL H., WESTERMANN R.: Interactive separating streak surfaces. *IEEE TVCG 16*, 6 (2010), 1569–1577. 2, 7

[Hal01] HALLER G.: Distinguished material surfaces and coherent structures in three-dimensional fluid flows. *Physica D 149*, 4 (2001), 248–277. 2, 3

[HH91] HELMAN J., HESSELINK L.: Visualizing vector field topology in fluid flows. *IEEE Computer Graphics and Applications 11* (May 1991), 36–46. 2

[HSW11] HLAWATSCH M., SADLO F., WEISKOPF D.: Hierarchical line integration. *IEEE TVCG 17*, 8 (2011), 1148–1163. 10

[Hul92] HULTQUIST J.: Constructing stream surfaces in steady 3D vector fields. In *IEEE Visualization* (1992), pp. 171–177. 7

[KGJ09] KRISHNAN H., GARTH C., JOY K.: Time and streak surfaces for flow visualization in large time-varying data sets. *IEEE TVCG 15*, 6 (2009), 1267–1274. 2, 7

[Pei09] PEIKERT R.:, 2009. private communication. 8

[Pop04] POPINET S.: Free computational fluid dynamics. *ClusterWorld 2*, 6 (June 2004). 7

[PR99] PEIKERT R., ROTH M.: The parallel vectors operator - a vector field visualization primitive. In *Proc. IEEE Visualization* (1999), pp. 263–270. 1, 2, 8

[SH95] SUJUDI D., HAIMES R.: *Identification of swirling flow in 3D vector fields*. Tech. rep., Department of Aeronautics and Astronautics, MIT, 1995. AIAA Paper 95-1715. 2, 8

[STW*06] SHI K., THEISEL H., WEINKAUF T., HAUSER H., HEGE H.-C., SEIDEL H.-P.: Path line oriented topology for periodic 2D time-dependent vector fields. In *Proc. EuroVis* (2006), pp. 139–146. 8

[TSW*05] THEISEL H., SAHNER J., WEINKAUF T., HEGE H.-C., SEIDEL H.-P.: Extraction of parallel vector surfaces in 3D time-dependent fields and application to vortex core line tracking. In *Proc. IEEE Visualization* (2005), pp. 631–638. 8

[vFWTS08] VON FUNCK W., WEINKAUF T., THEISEL H., SEIDEL H.-P.: Smoke surfaces: An interactive flow visualization technique inspired by real-world flow experiments. *IEEE TVCG 14*, 6 (2008), 1396–1403. 2, 7

[WCW*11] WIEBEL A., CHAN R., WOLF C., ROBITZKI A., STEVENS A., SCHEUERMANN G.: Topological flow structures in a mathematical model for rotation-mediated cell aggregation. In *Topological Methods in Data Analysis and Visualization*. Springer, 2011, pp. 193–204. 7, 8

[WSTH07] WEINKAUF T., SAHNER J., THEISEL H., HEGE H.-C.: Cores of swirling particle motion in unsteady flows. *IEEE TVCG 13*, 6 (2007), 1759–1766. 1, 2, 8

[WT02] WEINKAUF T., THEISEL H.: Curvature measures of 3D vector fields and their applications. *Journal of WSCG 10*, 2 (2002), 507–514. 1, 2

[WT10] WEINKAUF T., THEISEL H.: Streak lines as tangent curves of a derived vector field. *IEEE TVCG 16*, 6 (2010), 1225–1234. 2, 3, 5, 6, 8, 9

[WTS*07] WIEBEL A., TRICOCHE X., SCHNEIDER D., JAENICKE H., SCHEUERMANN G.: Generalized streak lines: Analysis and visualization of boundary induced vortices. *IEEE TVCG 13*, 6 (2007), 1735–1742. 6